

---

# Gas and Particle Motion

Paul A. Baron

*National Institute for Occupational Safety and Health  
Centers for Disease Control, Public Health Service  
Department of Health and Human Services, Cincinnati, OH, U.S.A.*

and

Klaus Willeke

*Department of Environmental Health  
University of Cincinnati  
Cincinnati, OH, U.S.A.*

## INTRODUCTION

Aerosols consist of two components: a gas or gas mixture, most commonly air, and the particles suspended in it. The behavior of the particles within the aerosol depends to a large extent on the motion and intrinsic properties of the suspending gas. Submicrometer-sized particles, especially those  $< 0.1 \mu\text{m}$  diameter, are affected by the motion of individual gas molecules (the free molecular regime). Thus, the kinetic theory of gases is useful in understanding the behavior of these particles. Larger particles can be treated as being submerged in a continuous gaseous medium or, more broadly, a fluid (the continuum regime). The tools of gas or fluid dynamics are more useful for this size range. Intermediate-sized particles can usually be treated by an adjustment of equations from the continuum regime. This intermediate range is termed the transition or slip regime. Whether considering a molecular ensemble or a continuous fluid, the motion of the gas will largely dictate the behavior of the suspended particles. In this chapter, concepts and parameters that affect gas and particle motion will be dis-

cussed and quantified as migration and deposition parameters in specific force fields.

## BULK GAS MOTION

### Reynolds Number

When measuring an aerosol, elucidating the gas flow patterns is critical to understanding what happens to the aerosol in the environment, on its way into the sensor of the measuring instrument, or in the actual sensor. While the aerosol particles follow the overall gas flow, their trajectories can deviate from the gas flow due to various external forces as well as changes in gas direction and velocity. Gas motion can be visualized by observing the streamlines, i.e., tracing the motion of miniscule volumes of gas. Gas flowing around an aerosol particle can have the same flow streamline pattern as gas passing around a large object such as a basketball.

The equivalence of fluid motion for various-sized objects can be described in terms of the forces involved. The flow pattern, whether it is smooth or turbulent, is governed by the ratio of the inertial force of the gas to the

friction force of the gas moving over the surface. This ratio is expressed by the Reynolds number,  $Re$ , an extremely useful parameter when dealing with aerosols:

$$Re = \frac{\rho_g V d}{\eta} = \frac{V d}{\nu} \quad (3-1)$$

where  $V$  is the velocity of the gas,  $\eta$  the dynamic gas viscosity,  $\nu$  the kinematic viscosity ( $= \eta/\rho_g$ ), and  $d$  a characteristic dimension of the object, such as the diameter of a sphere. Since this dimensionless number characterizes the flow, it depends on gas density,  $\rho_g$ , and not on the particle density. At normal temperature and pressure (NTP), i.e., 20°C (293 K) and 101 kPa (1 atm),  $\rho_g = 1.192 \times 10^{-3} \text{ g/cm}^3$  and  $\eta = 1.833 \times 10^{-4} \text{ dyn s/cm}^2$ , which reduces Eq. 3-1 to

$$Re = 6.5 V d \quad (3-2)$$

for  $V$  in cm/s and  $d$  in cm.

A distinction must be made between the flow Reynolds number,  $Re_f$ , and the particle Reynolds number  $Re_p$ . The flow Reynolds number defines the gas flow in a tube or channel of cross-sectional dimension  $d$ . The particle Reynolds number defines the gas flow around a particle that may be found in this tube or channel flow. The characteristic dimension in the latter is particle diameter,  $d_p$ , and  $V$  expresses the relative velocity between the particle and the gas flow. Since the difference between these velocities is generally small, and the particle's dimension is very small, the particle Reynolds number usually has a very small numerical value.

### Common Gas Flows

When friction forces dominate the flow, i.e., at low Reynolds numbers, the flow is smooth, or laminar. Under laminar flow, no streamlines loop back on themselves. At higher Reynolds numbers, the inertial forces dominate and loops appear in the streamlines until at still higher Reynolds numbers the flow becomes chaotic, or turbulent. The actual values of the

Reynolds number depend on how the gas flow is bounded. For instance, laminar flow occurs in a circular duct when the flow Reynolds number is less than about 2000, while turbulent flow occurs for Reynolds numbers above 4000. In the intermediate range, the gas flow is sensitive to the previous history of the gas motion. For instance, if the gas velocity is increased into this intermediate range slowly, the flow may remain laminar. When a gas passes around a suspended object, such as a sphere, flow is laminar for particle Reynolds numbers below about 0.1.

Since, often, it is expensive and difficult to test collection and measurement systems at full scale and *in situ*, small-scale water (or other liquid) models operating at the same Reynolds number as the system being studied are a useful alternative. Dye injection into the flow stream allows visualization of the streamlines. Such models can operate on a smaller physical scale with a slower time response, so that it is easy to observe the time evolution of flow patterns. The same technique can be used to model the behavior of particles.

### Example 3-1

Silica dust of 10  $\mu\text{m}$  diameter is removed by a 30 cm diameter ventilation duct at 2000 cm/s (about 4000 fpm). An old rule of thumb in industrial hygiene is that silica dust of this size gravitationally settles at 1 cm/s. Calculate the flow and particle Reynolds numbers at 20°C.

*Answer.* The relevant parameters for the flow Reynolds number are the duct diameter and the gas flow velocity in the duct. From Eq. (3-2),

$$\begin{aligned} Re_f &= 6.5 V d = 6.5(2000 \text{ cm/s})(30 \text{ cm}) \\ &= 3.9 \times 10^5 \end{aligned}$$

The relevant parameters for the particle Reynolds number are the particle diameter and the gravitational-settling velocity perpen-

directional to the gas flow:

$$Re_p = 6.5 Vd = 6.5(1.0 \text{ cm/s})(10 \times 10^{-4} \text{ cm}) \\ = 6.5 \times 10^{-3}$$

The flow Reynolds number exceeds 4000, indicating turbulent flow in the ventilation duct. The particle Reynolds number is less than one, indicating that the flow around the particle can be laminar. However, it is not so in this case because the gas flow is turbulent.

Many gas-handling systems for instruments use cylindrical tubing to carry the aerosol from one place to another. Understanding the flow patterns within the tubing is important for predicting the losses that occur within the tubing as well as predicting the distribution of particles within the tubing. If a gas begins to flow in a cylindrical tube, the friction at the wall slows the gas velocity relative to the motion at the center of the tube. At low Reynolds numbers, the dominating friction force produces a characteristic laminar parabolic velocity profile. The gas velocity at the center of the tube for this "Poiseuille flow" is twice that of the average velocity in the tube. Poiseuille flow does not get established immediately. A common rule of thumb is to assume that it takes ten tube diameters for this equilibrium flow to be effectively established.

The region near a surface where the flow is dominated by frictional forces is termed the boundary layer. When the flow starts along a surface, either in time or space, the boundary layer consists only of the gas at the surface, where the relative velocity is zero. At low Reynolds numbers, the boundary layer grows until steady-state conditions are reached. For the cylinder flow example above, the boundary layer grows into a parabolic flow profile that fills the cylinder, as indicated in the lower part of Fig. 3-1. At higher Reynolds numbers (in the turbulent regime) or during abrupt changes in flow conditions, the boundary layer can become separated from the surface. The development of the boundary layer and its relationship to the overall flow depends upon the object immersed in the fluid. This

type of behavior has been described in many fluid mechanics texts (e.g., White 1986) and especially in *Boundary-Layer Theory* by Schlichting (1979).

There are a wide variety of flow situations for which empirical or experimentally verified theoretical solutions exist. For instance, when a gas passing through a cylindrical tube under laminar flow conditions negotiates a 90° bend, the cylindrical symmetry of the flow pattern in the tube is reduced to a plane of symmetry. Thus, the flow symmetry must also be reduced. Two parallel circulation patterns are set up on either side of the plane of the bend, as shown in Fig. 3-1. This secondary pattern causes mixing of the gas as well as increased inertial forces on particles suspended in the gas (Tsai and Pui 1990). In tubing used to transport aerosols, bends are generally undesirable because of increased particle loss.

For various reasons, there are often constrictions or expansions in a tube carrying a gas. A constriction will force the gas to increase in velocity and be focused at the center of the tubing, even more than the constriction in size. After this contraction region, or "vena contracta," the gas flow eventually expands again to fill the tubing and reestablishes an equilibrium pattern. These disturbances will also cause increased particle deposition.

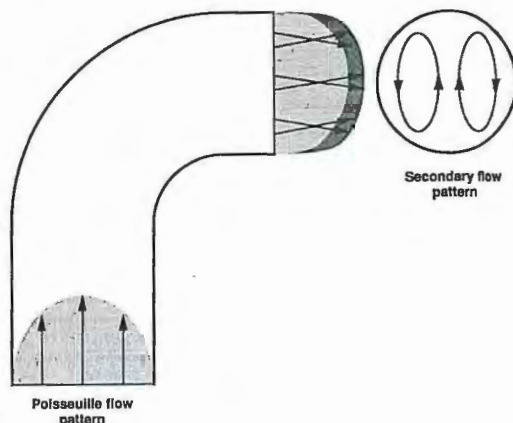


FIGURE 3-1. Flow Circulation After a 90° Bend in Tubing.

When a gas flows from an initial tube diameter into a suddenly expanded section or into free space, the flow pattern may persist for many initial tube diameters downstream. If the expansion of the tube is very slight, the flow does not separate from the walls and the flow pattern can expand smoothly to fill the increased diameter of the tube. In general, the angle between the wall and the tube axis needs to be less than 7° to avoid flow separation from the tube wall.

**Gas Density and Mach Number**

The density of a gas,  $\rho_g$ , is related to its temperature,  $T$ , and pressure,  $P$ , through the equation of state

$$P = \rho_g \frac{R_u}{M} T = \rho_g R T \tag{3-3}$$

where  $\rho_g$  is the gas density ( $= 1.192 \times 10^{-3}$  g/cm<sup>3</sup> for air at NTP),  $T$  is the absolute gas temperature in K,  $M$  is the molecular weight in g/mol and  $R_u$  is the universal gas constant ( $= 8.31 \times 10^7$  dyn cm/mol K). In air, the effective molecular weight is 28.9 g/mol. Thus, the specific gas constant for air is  $R = 2.88 \times 10^6$  dyn cm/K g or 2.84 atm cm<sup>3</sup>/K g. One atmosphere equals 101 kPa, where 1 Pa = 1 N/m<sup>2</sup> = 10 dyn/cm<sup>2</sup>.

When this gas moves at a high velocity relative to the acoustic velocity,  $U_g$ , in that gas, the gas becomes compressed. The degree of compression depends on the Mach number,  $Ma$ :

$$Ma = \frac{U}{U_{sonic}} \tag{3-4}$$

Here the gas velocity is designated as  $U$  to distinguish it from particle velocity  $V$ . When  $Ma \ll 1$ , the gas flow is considered incompressible. This is true in most aerosol sampling situations. In air, the sonic or sound velocity at ambient temperature is about 340 m/s (1100 ft/s).

**TRANSITION AND GAS MOLECULAR FLOW**

**Knudsen Number**

Large aerosol particles are constantly bombarded from all directions by a large number of gas molecules. When a particle is small, less than 1 μm in size, its location in space may be affected by the bombardment of individual gas molecules. Its motion is then no longer determined by continuum flow considerations, but by gas kinetics.

The average velocity of a molecule,  $\bar{V}$ , is a function of its molecular weight,  $M$ , and the gas temperature,  $T$ . In air ( $M_{air} = 28.9$  g/mol) at normal temperature and pressure (NTP, 20°C, 1 atm), this molecular velocity is 463 m/s. Using these air reference values, the average velocity can be estimated for other gases and temperatures:

$$\bar{V} = \bar{V}_r \left( \frac{T}{T_r} \right)^{1/2} \left( \frac{M_r}{M} \right)^{1/2} \tag{3-5}$$

The mean free path,  $\lambda$ , is the mean distance a molecule travels before colliding with another molecule. In air at 20°C and atmospheric pressure, the mean free path,  $\lambda_r$ , is 0.0665 μm. The mean free path is an abstraction that is determined from a kinetic theory model which relates it to the coefficient of viscosity. Using these reference values,  $\lambda$  is determined for other pressures and temperatures (Willeke 1976):

$$\lambda = \lambda_r \left( \frac{101.3}{P} \right) \left( \frac{T}{293.15} \right) \left( \frac{1 + 110/293.15}{1 + 110/T} \right) \tag{3-6}$$

where  $P$  is in kPa,  $T$  is in K, and  $S$  (in K) is the Sutherland constant (Table 3-1). If the unit of atmosphere is used for pressure, the factor of 101 used in Eq. (3-6) is substituted by one. The mean free path and the average molecular velocity are parameters that are frequently used to predict bulk properties of a gas, such as thermal conductivity, diffusion, and viscosity. Mean free paths for other gases are presented in Table 3-1.

**TABLE 3-1 Gas Properties for Several Gases at NTP (293.15 K and 101.3 kPa)**

Gas	$\eta$ ( $\mu\text{P}$ )	$S$ (K)	$\rho_g$ ( $10^{-3} \text{ g/cm}^3$ )	$\lambda$ ( $\mu\text{m}$ )
Air	182.03	110.4	1.205	0.0665
Ar	222.92	141.4	1.662	0.0694
He	195.71	73.8	0.167	0.192
H <sub>2</sub>	87.99	66.7	0.835	0.123
CH <sub>4</sub>	109.77	173.7	0.668	0.0537
C <sub>2</sub> H <sub>6</sub>	92.49	223.2	1.264	0.0328
iso-C <sub>4</sub> H <sub>10</sub>	74.33	255.0	2.431	0.0190
N <sub>2</sub> O	146.46	241.0	1.837	0.0433
CO <sub>2</sub>	146.73	220.5	1.842	0.0432

Source: Rader (1990).

The Knudsen number,  $Kn$ , relates the gas molecular mean free path to the physical dimension of the particle, usually the particle radius:

$$Kn = \frac{2\lambda}{d_p} \quad (3-7)$$

where  $d_p$  is the physical diameter of the particle. The Knudsen number is somewhat counterintuitive as an indicator of particle size since it has an inverse size dependence.  $Kn \ll 1$  indicates continuum flow and  $Kn \gg 1$  indicates free molecular flow. The intermediate range, approximately  $Kn = 0.4-20$ , is usually referred to as the transition or slip flow regime.

### Slip Flow Regime and Correction Factor

If a particle is much smaller than the gas molecular mean free path ( $Kn \gg 1$ ), it can travel past an obstacle at a very small distance from the object since no gas molecule may impede it. If the particle is very large ( $Kn \ll 1$ ), many gas molecular collisions occur near the surface and the particle is decelerated. When the Knudsen number is of the order of unity, the particle may slip by the obstacle. When the particle size is in this "slip flow regime," it is convenient to assume that the particle is still moving in a continuum gas flow. To accommodate the difference, a slip correction factor,  $C_c$ , also referred to as the

"Cunningham slip correction factor," is introduced into the equations. An empirical fit to air data for particles gives (Allen and Raabe 1985)

$$C_c = 1 + Kn[\alpha + \beta \exp(-\gamma/Kn)] \quad (3-8)$$

Various values for  $\alpha$ ,  $\beta$ , and  $\gamma$  have been reported. However, it is important to use the mean free path with which these constants were determined. The value of  $\lambda_r$  used in Eq. 3-6 should also be consistent with the derivation of the slip coefficient constants. For solid particles,  $\alpha = 1.142$ ,  $\beta = 0.558$ , and  $\gamma = 0.999$  (Allen and Raabe 1985). For oil droplets,  $\alpha = 1.207$ ,  $\beta = 0.440$ , and  $\gamma = 0.596$  (Rader 1989).  $C_c$  for other gases such as CO<sub>2</sub> and He are similar within a few percent. The slip correction and viscosity values are better determined than most other aerosol-related parameters and are, therefore, reported with a higher degree of precision.

For pressures other than atmospheric, the slip correction changes because of the pressure dependence of mean free path in  $Kn$  and the following may be used for solid particles:

$$C_c = 1 + \frac{1}{Pd_p} [15.39 + 7.518 \exp(-0.0741Pd_p)] \quad (3-9)$$

where  $P$  is pressure in kPa and  $d_p$  is the particle diameter in  $\mu\text{m}$  (Hinds 1982).

$C_c$  equals one in the continuum regime and and becomes greater than one for decreasing particle diameter in the transition regime. For instance,  $C_c = 1.02$  for 10  $\mu\text{m}$  particles, 1.15 for 1  $\mu\text{m}$  particles and 2.9 for 0.1  $\mu\text{m}$  particles. Note that the shape factor and the slip correction factor must be consistent with the type of equivalent diameter used in the same equation (Brockmann and Rader 1990).

### Gas Viscosity

Gas viscosity is primarily due to the momentum transfer that occurs during molecular collisions. These frequent and rapid collisions tend to damp out differences in

bulk gas motion as well as impede the net motion of particles relative to the gas. Thus, the mobility of a particle in a force field depends on the aerodynamic drag exerted on the particle through the gas viscosity. Fluid dynamic similitude, as expressed by the Reynolds number, depends on gas viscosity,  $\eta$ . Therefore, a knowledge of the gas viscosity is important when dealing with aerosol particle mechanics. The viscosity can be related to a reference viscosity,  $\eta_r$ , and a reference temperature,  $T_r$ , as:

$$\eta = \eta_r \left( \frac{T_r + S}{T + S} \right) \left( \frac{T}{T_r} \right)^{3/2} \quad (3-10)$$

where  $S$  is the Sutherland interpolation constant (Schlichting 1979). Note that viscosity is independent of pressure.

In cgs units, viscosity is expressed in dyn s/cm<sup>2</sup>, also referred to as poise or P. For air at 293.15 K, the viscosity is 182.03  $\mu$ P and  $S = 110.4$  K. The interpolation formula is fitted to the data over the range 180–2000 K (Schlichting 1979). Reference values of viscosity and Sutherland constants for other gases are presented in Table 3-1.

## GAS AND PARTICLE DIFFUSION

The random movement of gas molecules causes gas and particle diffusion if there is a concentration gradient. For instance, in a diffusion denuder, SO<sub>2</sub> gas molecules may diffuse to an absorbing surface due to their high diffusivity. Sulfate particles, which are larger and, therefore, have lower diffusivity, will mostly be transported through the device. Thus, the SO<sub>2</sub> gas molecules are separated from the sulfate particles.

### Gas Diffusion

Diffusion always causes net movement from a higher concentration to a lower one. The net flux of gas molecules,  $J$ , is in the direction of lower concentration. Thus, in simple one-

dimensional diffusion,

$$J = -D \frac{\partial N}{\partial x} \quad (3-11)$$

where  $x$  is the direction of diffusion,  $N$  is the concentration, and  $D$  is a proportionality constant, referred to as the diffusion coefficient. The diffusion coefficient for a gas with molecular weight  $M$  is (Hinds 1982, 24)

$$D = - \left( \frac{3\sqrt{2}\pi}{64Nd_{\text{molec}}^2} \right) \sqrt{\frac{RT}{M}} \quad (3-12)$$

where  $N$  is the number of gas molecules/cm<sup>3</sup> and  $d_{\text{molec}}$  is the molecular collision diameter ( $3.7 \times 10^{-8}$  cm for air). The diffusion coefficient of air molecules at 293 K is 0.18 cm<sup>2</sup>/s.

### Particle Diffusion

Small particles can achieve significant diffusive motion in much the same fashion as described for gas molecules. The difference is only in the particle size and shape. Because of their increase in inertia with particle mass and the larger surface area over which the bombardment by the gas molecules is averaged, large particles will diffuse more slowly than small particles. For particles in a gas, the diffusion coefficient or diffusivity,  $D$ , can be computed by

$$D = \frac{kTC_c}{3\pi\eta d_p} = kTB \quad (3-13)$$

where  $k$ , the Boltzmann constant, is  $1.38 \times 10^{-16}$  dyn cm/K and the mechanical mobility,  $B$  (cm/s dyn), is a convenient aerosol property that combines particle size with some of the properties of the suspending gas:

$$B = \frac{C_c}{3\pi\eta d_p} \quad (3-14)$$

Particle diffusion, also referred to as Brownian motion, occurs because of the relatively high velocity of small particles and it is sometimes useful to estimate how far, on an

average, these particles move in a given time. The root mean square (rms) distance,  $x_{\text{rms}}$ , that the particles can travel in time  $t$  is

$$x_{\text{rms}} = \sqrt{2Dt} \quad (3-15)$$

### Example 3-2

Fume aerosols of  $0.01 \mu\text{m}$  diameter are drawn into the deep lung regions of a worker whose alveoli can be approximated by  $0.2 \text{ mm}$  diameter spheres. Estimate if these particles are likely to deposit in this area of the lung during a breath-holding period of  $4 \text{ s}$ . Assume the body temperature to be  $37^\circ\text{C}$ .

*Answer.* We note that calculation of  $x_{\text{rms}}$  (Eq. 3-15) requires a knowledge of the diffusion coefficient, which in turn requires the slip correction factor and viscosity. To simplify the calculation, let us assume for the moment that diffusion is taking place at room temperature. Thus, the air viscosity is  $183 \mu\text{P}$  and the mean free path is  $0.0665 \mu\text{m}$ . (For a more exact estimate of these parameters at body temperature, use Eqs. 3-6 and 3-10, respectively.)

The slip correction factor can be determined from Eq. 3-8 using constants for solid particles:

$$C_c = 1 + Kn[1.142 + 0.558 \exp(-0.999/Kn)]$$

$$C_c = 1 + \frac{2 \times 0.0665 \mu\text{m}}{0.01 \mu\text{m}} \left[ 1.142 + 0.558 \exp\left(-0.999 \frac{0.01 \mu\text{m}}{2 \times 0.0665 \mu\text{m}}\right) \right]$$

$$= 23.1$$

We then estimate the diffusion coefficient, using Eq. 3-13.

$$D = \frac{kTC_c}{3\pi\eta d_p}$$

$$D = \frac{(1.36 \times 10^{-16} \text{ dyn cm/K})(293 \text{ K})(23.1)}{3 \times 3.14(1.83 \times 10^{-4} \text{ P})(1 \times 10^{-6} \text{ cm})}$$

$$= 5.33 \times 10^{-4} \text{ cm}^2/\text{s}$$

Finally, using Eq. 3-15,

$$x_{\text{rms}} = \sqrt{2Dt} = \sqrt{2(5.33 \times 10^{-4} \text{ cm}^2/\text{s})(4 \text{ s})}$$

$$= 0.0653 \text{ cm} = 0.653 \text{ mm}$$

We find that at room temperature, the rms displacement by diffusion is much larger than the alveolar size. At the elevated temperature in the lung ( $37^\circ\text{C}$ ), the particles are expected to move faster and diffuse further. If this air temperature is used in the calculation of the diffusion coefficient,  $x_{\text{rms}}$  is  $0.697 \text{ mm}$ . Thus, we know that most of these particles are likely to be collected in the alveolar space of the lung. A more exact analysis can be made by considering such factors as the spherical geometry of the alveoli, the location of the particles within the alveoli, and the air temperature.

By including the air temperature dependence also in the calculation of viscosity and mean free path, the rms displacement calculation results in  $0.681 \text{ mm}$ .

Table 3-2 includes examples of  $x_{\text{rms}}$  for various sized particles after a period of  $10 \text{ s}$ .

### Peclet Number

The amount of convective transport of particles towards an object may be related to the diffusive transport through the dimensionless Peclet number,  $Pe$ :

$$Pe = \frac{Ud_c}{D} \quad (3-16)$$

where  $d_c$  is the significant dimension of the particle-collecting surface and  $U$  is the upstream gas velocity towards the surface. The larger the value of  $Pe$ , the less important is the diffusional process (Licht 1988, 226).  $Pe$  is often used in the description of diffusional deposition on filters.

### Schmidt Number

The ratio of the Peclet number (Eq. 3-16) to the Reynolds number (Eq. 3-1) is referred to

as the Schmidt number,  $Sc$ . It expresses the ratio of kinematic viscosity to diffusion coefficient:

$$Sc = \frac{\eta_g}{\rho_g D} = \frac{\nu}{D} \quad (3-17)$$

As the Schmidt number increases, convective mass transfer increases relative to Brownian diffusion of particles. It has been used for describing diffusive transport in flowing fluids (convective diffusion), especially in the development of filtration theory (Friedlander 1977).  $Sc$  is relatively independent of temperature and pressure near standard conditions.

## AERODYNAMIC DRAG ON PARTICLES

Externally applied forces on an aerosol particle are opposed and rapidly balanced by the aerodynamic drag force. An example of this is a sky diver: the gravitational force pulling the sky diver towards the earth is eventually balanced by the air resistance and the diver reaches a final falling speed of about 63 m/s (140 miles per hour).

A particle's drag force,  $F_{\text{drag}}$ , relates the resistive pressure of the gas to the velocity pressure and is determined by the relative motion between the particle and the surrounding gas. When the particle dimensions are much larger than the distance between the gas molecules, the surrounding gas can be considered as a continuous fluid (continuum regime). Under this condition, the drag force is given by

$$F_{\text{drag}} = \frac{\pi}{8} C_d \rho_g V^2 d_p^2 \quad (3-18)$$

Note that the aerodynamic drag is related to the gas density,  $\rho_g$ , and not the particle density. The drag coefficient,  $C_d$ , relates the drag force to the velocity pressure. When the inertial force pushing the gas aside, due to the velocity difference between the gas and the particle, is much smaller than the viscous resistance force, the drag coefficient,  $C_d$ , is expressed in terms of gas flow parameters:

$$C_d = \frac{24}{Re_p}, \quad Re_p < 0.1 \quad (3-19)$$

where  $Re_p$  is the particle Reynolds number. This relationship is accurate within 1% in the  $Re_p$  range indicated. If 10% accuracy is acceptable, Eq. 3-19 can be used up to  $Re_p < 1.0$ . Combining Eqs. 3-1, 3-18, and 3-19 results in

$$F_{\text{drag}} = 3\pi\eta \dot{V} d_p \quad (3-20)$$

This equation is also known as the Stokes law. For the Stokes law flow of gas around the particle, the drag on the particle depends only on gas viscosity,  $\eta$ , particle velocity,  $V$ , and particle diameter,  $d_p$ . This assumes that the particle is spherical. The particle drag for shapes other than spheres is usually difficult to predict theoretically. Therefore, for particles of other shapes, a dynamic shape factor,  $\chi$ , is introduced that relates the motion of the particle under consideration to that of a spherical particle

$$F_{\text{drag}} = 3\pi\eta\chi V d_m \quad (3-21)$$

where  $d_m$  is now the mass-equivalent diameter, defined as the diameter of a sphere composed of the particle bulk material with no voids that has the same mass as the particle in question. The shape factor is sometimes related to the equivalent volume or volume-equivalent diameter,  $d_{ev}$ , defined as the diameter of a sphere of equivalent volume. This term may be ambiguous. When the equivalent volume is composed of particle bulk material with no void,  $d_{ev} = d_m$ . However, if the material includes voids,  $d_{ev} > d_m$ . If we determine the shape factors and equivalent diameters for particles that we wish to measure, the behavior of the particles can be predicted when they are influenced by various force fields, e.g., gravity or electrostatic.

We know that gases are not continuous fluids as indicated above, but consist of discrete molecules. Therefore, when the particle size approaches the mean free path of the gas molecular motion (transition or slip regime), we can apply a correction that takes the "slip" between the particle and the gas into account. Thus, the Cunningham slip correction factor,

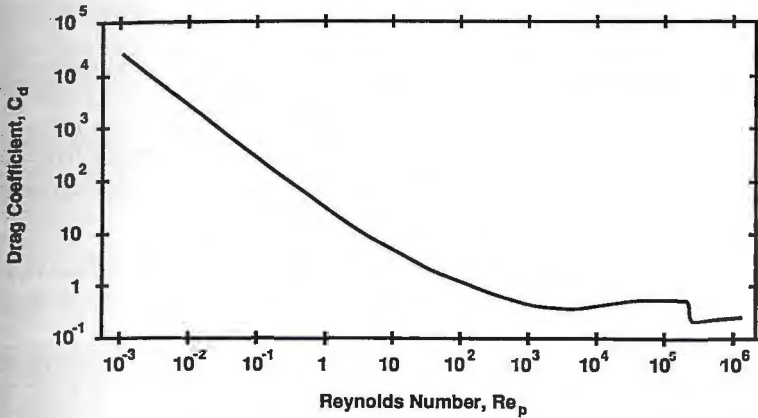


FIGURE 3-2. Drag Coefficient as a Function of Particle Reynolds Number for Spherical Particles.

$C_c$ , is introduced into Eq. 3-21:

$$F_{\text{drag}} = \frac{3\pi\eta\chi Vd_c}{C_c} \quad (3-22)$$

Equation 3-22 assumes that the flow around the particle is laminar. As particles move faster (i.e., have a larger  $Re_p$ ), the above relationships must be modified further. As indicated above, the range over which Eq. 3-19 is accurate defines the Stokes regime. For larger  $Re_p$ , empirical relationships for  $C_d$  have been developed to extend Stokes law. The drag coefficient,  $C_d$ , for a spherical particle is the ratio of the resistance pressure due to aerodynamic drag (drag force/cross-sectional area) to the velocity pressure of the flow towards the sphere, based on the relative velocity between the particle and the suspending gas. Figure 3-2 shows the relationship of the drag coefficient to the particle Reynolds number over a wide range of Reynolds numbers.

For  $Re_p$  above 0.1, Sartor and Abbott (1975) developed the following empirical relationship:

$$C_d = \frac{24}{Re_p}(1 + 0.0916Re_p), \quad 0.1 \leq Re_p < 5 \quad (3-23)$$

and Serafini (Friedlander 1977, 105), the fol-

lowing:

$$C_d = \frac{24}{Re_p}(1 + 0.158Re_p^{2/3}), \quad 5 \leq Re_p < 1000 \quad (3-24)$$

Note that these relationships have been derived from data taken with smooth spheres. Similar relationships have been derived and reviewed for particles such as droplets, solid spheroids, disks, and cylinders (Clift, Grace, and Weber 1978, 142). Typically,  $Re_p$  is based on the equatorial diameter for disks and spheroids and on the cylinder diameter for cylinders, although other definitions can be used. Particles with extreme shapes may have a significantly different drag coefficient. For instance,  $C_d$  for fibers is up to 4 times lower than for spheres with  $Re_p < 100$  when the fiber diameter is used as the significant dimension in the Reynolds number expression (Eq. 3-1).

Thus, by using the appropriate form of the drag coefficient (Eq. 3-19, 3-23, or 3-24) and including the shape factor and slip coefficient, the drag force can be calculated over a wide range of particles and conditions:

$$F_{\text{drag}} = \frac{\pi C_d \rho_g \chi V^2 d_p^2}{8C_c} \quad (3-25)$$

## PARTICLE MOTION DUE TO GRAVITY

The gravitational force,  $F_{\text{grav}}$ , is proportional to particle mass,  $m_p$ , and gravitational accel-

eration,  $g$ :

$$F_{\text{grav}} = m_p g = (\rho_p - \rho_g) v_g p \approx \rho_p v_p g \quad (3-26)$$

where  $\rho_g$  is the gas density. The gravitational pull depends on the difference between the density of the particle and that of the surrounding medium. For a particle in water, this buoyancy effect is significant. For a particle in air, the buoyancy effect can be neglected for compact particles since the particle density is generally much greater than the density of the gas. If the particle is spherical, particle volume,  $v_p$ , can be replaced with  $\pi d_p^3/6$ :

$$F_{\text{grav}} = \frac{\pi}{6} d_p^3 \rho_p g \quad (3-27)$$

The gravitational field of the earth was mentioned in Chapter 2. This field exerts a force pulling a particle down. As the particle begins to move, the gas surrounding the particle exerts an opposing drag force, which, after a short period of acceleration, equals the gravitational force and the particle reaches its terminal settling velocity. By equating the two forces, the following relationship is obtained for the gravitational-settling velocity,  $V_{\text{grav}}$ , in the Stokes regime (Eq. 3-19):

$$V_{\text{grav}} = V_{\text{ts}} = \frac{\rho_p d_p^2 g C_c}{18\eta}, \quad Re_p < 0.1 \quad (3-28)$$

In order to reflect the equilibrium between the two opposing forces, this velocity is also referred to as terminal settling velocity,  $V_{\text{ts}}$ . Assuming negligible slip ( $C_c = 1$ ), this equation reduces to the following at NTP:

$$V_{\text{grav}} = 0.003 \rho_p d_p^2 \quad (3-29)$$

where  $\rho_p$  is in  $\text{g/cm}^3$  and  $d_p$  in  $\mu\text{m}$ . Spherical particles (e.g., droplets) are common in nature and their motion can be described mathematically. Therefore, the behavior of nonspherical particles is often referenced to such particles through a comparison of their behavior in a gravitational field.

### Example 3-3

An open-faced filter cassette samples at 2 l/min ( $33.3 \text{ cm}^3/\text{s}$ ) over its inlet face of about 35 mm diameter. If the cassette is held facing downward, can a  $25 \mu\text{m}$  diameter particle with a density of  $3 \text{ g/cm}^3$  be drawn upward onto the filter in calm air?

*Answer.* The cassette samples at a flow rate  $Q$  over a cross-sectional filter area  $A$ . The upward air velocity,  $U$ , is

$$U = \frac{Q}{A} = \frac{33.3 \text{ cm}^3/\text{s}}{\pi \left(\frac{3.5 \text{ cm}}{2}\right)^2} = 3.46 \text{ cm/s}$$

The gravitational settling velocity of the  $25 \mu\text{m}$  particle is, from Eq. 3-29,

$$\begin{aligned} V_{\text{grav}} &= 0.003 \rho_p d_p^2 \\ &= 0.003(3 \text{ g/cm}^3)(0.0025 \text{ cm})^2 \\ &= 5.63 \text{ cm/s} > 3.46 \text{ cm/s} \end{aligned}$$

The particle cannot be drawn upward into the sampler.

This is also the principle of a vertical elutriator, which prevents particles above a certain size from passing through the device. However, in some implementations of this device, e.g., the cotton dust elutriator, inlet effects complicate the penetration efficiency.

The aerodynamic diameter,  $d_a$ , of a particle is the diameter of a unit-density sphere that has the same settling velocity as the particle in question, as shown in Eqs. 2-1–2-3 of Chapter 2. Another definition that is also commonly used is the Stokes diameter,  $d_s$ , which is the diameter of a spherical particle with the same density and settling velocity as the particle in question. The aerodynamic diameter can be related to the Stokes diameter through the settling velocity equation

$$\rho_p d_s^2 = 1 d_a^2 = d_a^2 \quad (3-30)$$

A number of instruments, including the horizontal and the vertical elutriators, use settling velocity to separate particles according to

size. For instance, aerosol particles of a certain size ( $d_p$ ), initially spread throughout a quiescent rectangular chamber or room of height  $H$ , will settle at a constant velocity,  $V_{\text{grav}}$ . After some time,  $t$ , the particle concentration in the chamber,  $N(t)$ , will be

$$N(t) = N_0 \left( 1 - \frac{V_{\text{grav}} t}{H} \right) \quad (3-31)$$

where  $n_0$  is the initial particle concentration in the chamber. The same relationship determines the concentration of particles in a rectangular channel with air flowing through it (a horizontal elutriator). At some distance downstream of the entrance to the channel (where the aerosol concentration is  $n_0$ ), the concentration will be  $n(t)$ , where  $t$  is the time needed to reach that distance.

The above discussion of particle settling describes the behavior of particles in still air, a condition that is not often achieved in the environment or even in the laboratory. When the gas in a container undergoes continual and random motion, such as in a room with several randomly directed fans, the particles undergo "stirred settling." The time-dependent concentration,  $n(t)$ , under these conditions is also expressed in terms of an initial particle concentration,  $n_0$ , the gravitational-settling velocity in still air,  $V_{\text{grav}}$ , and the height of the container,  $H$ :

$$N(t) = N_0 \exp\left(-\frac{V_{\text{grav}} t}{H}\right) \quad (3-32)$$

This equation applies to any container shape with vertical walls and a horizontal bottom. This indicates that even under stirred or turbulent conditions, larger particles (higher settling velocities) will settle down more rapidly than smaller particles, even though some of the large particles may persist in the air for a long time because of the exponential decay. Note that the form of Eqs. 3-31 and 3-32 are similar except for the exponential decay when stirring takes place during the settling. This similarity in form occurs for all such comparisons of uniform and stirred settling.

### Gravitational Settling at Higher Reynolds Numbers

Particle-settling velocity can be calculated accurately for  $Re_p < 0.1$  using Eq. 3-28. At higher Reynolds numbers, the observed settling velocity is lower than predicted by this equation because the drag coefficient is higher than predicted by Eq. 3-19. For spherical particles ( $\chi = 1$ ), the gravitational-settling velocity can be expressed as a function of  $C_d$  by equating the drag force (Eq. 3-25) to the gravitational force (Eq. 3-27):

$$V_{\text{grav}} = \sqrt{\frac{4 \rho_p C_c d_p g}{3 \rho_g C_d \chi}} \quad (3-33)$$

The drag coefficient has a complex dependence on the settling velocity and, therefore, Eq. 3-33 cannot be solved in closed form. Graphical (Licht 1988, 160) and tabular (Hinds 1982, 51) determinations of the settling velocity at high Reynolds numbers have been used. Using Eq. 3-33 and the drag coefficient equation for the appropriate Reynolds number, e.g., Eq. 3-23 or 3-24, an iterative solution for the settling velocity can readily be obtained using a computer or calculator. A guess for  $C_d$  allows the calculation of an initial value for  $V_{\text{grav}}$ , which is then used to calculate a new value of  $C_d$ . The new value of  $C_d$  is then used in Eq. 3-33 and the iteration is continued until the values converge.

### PARTICLE PARAMETERS

The gravitational force effectively removes large particles from the suspending gas. Particles of  $1 \mu\text{m}$  or smaller take a long time to settle (see Table 3-2). To settle these, the removal force is increased, e.g., by rotating the gas volume, as in a centrifuge. Other devices channel the gas flow in a circular fashion (e.g., cyclones) or through bends (e.g., impactors) to create an increased force field. The following parameters are useful for describing the inertial and settling behavior of particles.

**Relaxation Time and Stopping Distance**

Using the Stokes settling velocity relationship (Eq. 3-28), several useful particle parameters can be defined. The first is the particle relaxation time,

$$\tau = \frac{\rho_p d_p^2 C_c}{18\eta} \tag{3-34}$$

This is the time a particle takes to reach 1/e of its final velocity when subjected to a gravitational field. The relaxation period is typically quite short, as indicated in Table 3-2, and can, therefore, be neglected for most practical applications. Use of this parameter simplifies the expression for gravitational settling to

$$V_{grav} = \tau g \tag{3-35}$$

Quite often, a particle, rather than starting from rest in a gravitational field, is injected into the air with an initial velocity,  $V_0$ . For instance, such a particle might be released from a rotating grinding wheel. The product of the relaxation time and the initial particle velocity is referred to as the stopping distance,  $S$ :

$$S = V_0 \tau \tag{3-36}$$

where  $S$  is in cm. Values of  $S$  for an initial velocity of 1000 cm/s are given in Table 3-2. The concept of stopping distance is useful, e.g., in impactors when evaluating how far a

particle moves across the air streamlines when the flow makes a right-angle bend.

**Example 3-4**

A grinding wheel dislodges many wheel and workpiece particles and projects them from the contact point towards the receiving hood of the ventilation system. A particle of a certain size and density is projected 1 cm away. How far will a particle twice this size be projected? Estimate the projected distance when the speed of the grinding wheel is doubled.

*Answer.* The projected distance is proportional to the stopping distance. From Eqs. 3-34 and 3-36,

$$S = V_0 \tau \propto V_0 \rho_p d_p^2$$

The stopping distance depends on the square of the particle diameter, so a two-times-larger particle will project the distance four times, to 4 cm. At twice the grinding wheel speed, the particle will come off at approximately twice the initial velocity, resulting in a doubling of the distance to 2 cm.

The above stopping distance equation assumes that the particle is in the Stokes regime. If the particle diameter and velocity are such that  $Re_p$  is larger than 0.1, the stopping distance will be somewhat less than quadrupled for the larger particle. This is because outside

**TABLE 3-2 Particle Parameters for Unit-Density Particles Under Standard Conditions**

Particle Diameter, $d_p$ ( $\mu\text{m}$ )	Slip Correction Factor, $C_c$	Settling Velocity, $V_{grav}$ (cm/s)	Relaxation Time, $\tau$ (s)	Stopping Distance, $S$ $V_0 = 1000$ cm/s (cm)	Mobility, $B$ (cm/dyn s)	Diffusion Coefficient, $D$ ( $\text{cm}^2/\text{s}$ )	rms Brownian Displacement in 10s (cm)
0.00037 <sup>a</sup>			$2.6 \times 10^{-10}$	$2.5 \times 10^{-7}$	$9.7 \times 10^{12}$	0.18 <sup>b</sup>	2.80
0.01	23.04	$6.95 \times 10^{-6}$	$7.1 \times 10^{-9}$	$7.1 \times 10^{-6}$	$1.4 \times 10^{10}$	$5.5 \times 10^{-4}$	0.10
0.1	2.866	$8.65 \times 10^{-5}$	$8.8 \times 10^{-8}$	$8.8 \times 10^{-5}$	$1.7 \times 10^8$	$6.8 \times 10^{-6}$	$1.2 \times 10^{-2}$
1	1.152	$3.48 \times 10^{-3}$	$3.5 \times 10^{-6}$	$3.5 \times 10^{-3}$	$6.8 \times 10^6$	$2.7 \times 10^{-7}$	$2.3 \times 10^{-3}$
10	1.015	$3.06 \times 10^{-1}$	$2.3 \times 10^{-4}$	0.23	$6.0 \times 10^5$	$2.4 \times 10^{-8}$	$7.0 \times 10^{-4}$
100	1.002	$2.61 \times 10^1$	$1.3 \times 10^{-2}$	13	$5.9 \times 10^4$	$2.4 \times 10^{-9}$	$2.2 \times 10^{-4}$

a. Average diameter of a molecule in air

b. Calculated using Eq. 3-12

the Stokes regime the drag increases faster with diameter (see Fig. 3-2). Similarly, increasing the initial velocity also increases  $Re_p$  and results in somewhat less than doubling of the distance.

Since Eq. 3-28 is accurate only in the Stokes regime, the following empirical relationship can be used at higher  $Re_p$  (Mercer 1973, 41):

$$S = \frac{\rho_p d_p}{\rho_g} \left[ Re_0^{1/3} - \sqrt{6} \arctan \left( \frac{Re_0^{2/3}}{\sqrt{6}} \right) \right],$$

$$1 < Re_p < 400 \quad (3-37)$$

where  $Re_0$  is the Reynolds number of the particle at the initial velocity.

### Stokes Number

When gas flow conditions change suddenly, as at the particle collection surface of an impactor, the ratio of the stopping distance to a characteristic dimension,  $d$ , is defined as the Stokes number,  $Stk$ :

$$Stk = \frac{S}{d} \quad (3-38)$$

The characteristic dimension depends on the application, e.g., in fibrous filtration it is the diameter of the fiber and in impaction flows it is the radius of the impactor nozzle. For a given percentage of particle removal, the Stokes number value is, therefore, application-specific. For example, the Stokes number of an impactor with one or several identical circular nozzles is

$$Stk = \frac{\rho_p d_p^2 V C_c}{9 \eta d_j} \quad (3-39)$$

where  $d_j$  is the impactor jet diameter in cm and  $V$  is the particle velocity in the jet.  $V$  is assumed to be equal to the gas velocity in the jet.

### Shape Factor

As described above, particle aerodynamic diameter and the Stokes diameter have been

defined using ideal spherical particles. Apart from liquid droplets or particles produced from liquid droplets, few particles in nature are spheres. It is convenient to describe more complex shapes by a single diameter and have the additional flow resistance or drag represented by a factor. This dynamic shape factor,  $\chi$ , is the ratio of the drag force of the particle in question (particle diameter  $d_p$ ) to that of a sphere of equivalent volume (volume-equivalent diameter  $d_{ev}$ ). The expression for gravitational settling (Eq. 3-28) thus becomes

$$V_{grav} = \frac{\rho_p d_p^2 g C_c(d_p)}{18 \eta} = \frac{d_a^2 g C_c(d_a)}{18 \eta}$$

$$= \frac{\rho_p d_{ev}^2 g C_c(d_{ev})}{18 \eta \chi}, \quad Re_p < 0.1 \quad (3-40)$$

The value of the Cunningham slip factor,  $C_c$ , depends on the chosen diameter,  $d_p$ ,  $d_a$  or  $d_{ev}$ . The shape factor is always equal to or greater than one. Compact shapes typically have values between one and two, while more extreme shapes, such as fibers and high-volume aggregates, may have larger values. Shape factors are useful for converting a readily measurable equivalent diameter to one that depends on particle behavior, such as aerodynamic diameter or diffusion-equivalent diameter. Thus, shape factors have been defined in a variety of ways that have to do with the available means of measuring the physical and equivalent particle diameter as well as the means of measuring particle drag. Therefore, when applying published shape factors, it may be important to understand the experimental basis for their development.

Some particles have relatively regular shapes with volumes that can be calculated or compact shapes that can be measured with a microscope to determine a volume-equivalent diameter. For such particles, the shape factor is, from Eq. 3-40,

$$\chi = \frac{\rho_p d_{ev}^2 C_c(d_{ev})}{d_a^2 C_c(d_a)}, \quad Re_p < 0.1 \quad (3-41)$$

Three variables need to be measured:  $\rho_p$ ,  $d_{ev}$  and  $d_a$ . The volume-equivalent diameter may

be measured microscopically or determined from the mass (measured chemically or using radioactive tracers) and the number of particles (Barbe-le Borgne et al. 1986). The aerodynamic diameter can be measured in a settling chamber or centrifuge and, if the particle contains no voids, the density is the bulk density of the particle material.

Shape factors have also been measured by settling macroscopic models of regularly shaped particles in liquids. For instance, this technique has been used to measure shape factors for cylinders and chains of spheres (Kasper, Niida, and Yang 1985), for rectangular prisms (Johnson, Leith, and Reist 1986), and for modified rectangular prisms (Sheaffer 1987). These particles have two or three distinct symmetry axes and, therefore, may have two or three shape factors, depending on their orientation. Shape factors have also been derived for oblate and prolate spheroids (Fuchs 1964, 37). Table 3-3 exemplifies a few.

Porous particles, aggregates, and fume particles may have an effective density ( $\rho_e$ , including internal voids) that is quite different from the bulk material density,  $\rho_p$ . In this

case, a shape factor defined as a function of the mass-equivalent diameter ( $d_m$ ) may be more appropriate (Brockmann and Rader 1990), thus replacing  $d_{cv}$  with  $d_m$  in Eq. 3-41. The shape factor  $\chi$  may be further broken down as the product of envelope shape factor,  $\kappa$ , and a second component,  $\delta$  [defined as  $(\rho_p/\rho_e)^{1/3}$ ], which is due to the porosity of the particle. Theoretically or empirically derived shape factors as described above can be used to match the approximate envelopes of the observed particles. For relatively compact particles, the porosity component of  $\chi$  dominates, while for more sparse, branched-chain aggregates the envelope factor dominates.

## PARTICLE MOTION IN AN ELECTRIC FIELD

The application of electrostatic forces is particularly effective for submicrometer-sized particles, for which gravity forces are weak because of the  $d_p^3$  dependence (Eq. 3-27). On a large scale, removal of aerosols by electrostatic forces is practiced in electrostatic precipitators (also called electrofilters). In aerosol sampling and measuring instruments, electrostatic forces are applied to precipitate or redirect either all aerosol particles or those in a specific size range. Such particle motion caused by an electric field is called *electrophoresis*.

For a particle with a total charge equal to  $n$  times the elementary unit of charge,  $e$ , the electrostatic force,  $F_{elec}$ , in an electric field of intensity  $E$  is

$$F_{elec} = neE \quad (3-42)$$

### Example 3-5

A 0.5  $\mu\text{m}$  diameter unit density particle has been diffusion-charged with 18 elementary units of charge. Calculate the electrical force on the particle when it passes between two flat parallel plates (e.g., an electrostatic precipitator) which have 5 kV applied across a 2 cm gap. Compare the electrical to the gravitational force.

TABLE 3-3 Dynamic Shape Factors for Various Types of Compact Particles (No Internal Voids)

Shape	Dynamic Shape Factor, $\chi$
Sphere	1.00
Cluster of spheres	
2-sphere chain	1.12
3-sphere chain	1.27
4-sphere chain	1.32
Prolate spheroid ( $L/D = 5$ ) <sup>a</sup>	
Axis: horizontal	1.05
Axis: vertical	1.39
Glass fiber ( $L/D = 5$ )	1.71
Dusts	
Bituminous coal	1.05–1.11
High-ash soft coal	1.95
Quartz	1.36–1.82
Sand	1.57
Talc	2.04
$\text{UO}_2$	1.28
$\text{ThO}_2$	0.99

Source: Davies (1979)

a. Calculated values; all others are experimental

*Answer.* Expressed in cgs units, the electric field between the plates is

$$E = \left( \frac{5000 \text{ V}}{2 \text{ cm}} \right) \left( \frac{1 \text{ statV}}{300 \text{ V}} \right) = 8.33 \frac{\text{statV}}{\text{cm}}$$

Using Eq. 3-42,

$$\begin{aligned} F_{\text{elec}} &= neE \\ &= 18(4.8 \times 10^{-16} \text{ statC})(8.33 \text{ statV/cm}) \\ &= 7.2 \times 10^{-8} \text{ dyn} \end{aligned}$$

In SI units, the same calculation is:

$$\begin{aligned} E &= \frac{5000 \text{ V}}{2 \times 10^{-2} \text{ m}} = 2.5 \times 10^5 \frac{\text{V}}{\text{m}} \\ F_{\text{elec}} &= neE \\ &= 18(1.6 \times 10^{-16} \text{ C})(2 \times 10^5 \text{ V/m}) \\ &= 7.2 \times 10^{-13} \text{ N} \end{aligned}$$

One newton (N) in SI units equals  $10^5$  dyn in the cgs system of units. Using Eq. 3-27,

$$\begin{aligned} F_{\text{grav}} &= \frac{\pi}{6} d_p^3 \rho_p g \\ &= \frac{\pi}{6} (0.5 \times 10^{-4} \text{ cm})^3 \left( \frac{1 \text{ g}}{\text{cm}^3} \right) \left( 980 \frac{\text{cm}}{\text{s}^2} \right) \\ &= 6.41 \times 10^{-11} \text{ dyn} \end{aligned}$$

Comparing the two forces,

$$\frac{F_{\text{elec}}}{F_{\text{grav}}} = \frac{7.2 \times 10^{-8}}{6.41 \times 10^{-11}} = 1120$$

The electric force exceeds the gravity force by over a thousand times.

Electrostatic forces can affect particle motion, and to a certain extent, gas motion as well. These forces can be important during particle generation, transport, and measurement. If a particle is placed in an electric field described by Eq. 3-42, it will reach a terminal velocity,  $V_{\text{elec}}$ , when the field and drag forces are equal:

$$V_{\text{elec}} = \frac{neEC_c}{3\pi\eta d_p} \quad (3-43)$$

The electronic charge,  $e$ , is  $4.80296 \times 10^{-10}$  statcoulomb (statC). This terminal, or drift, velocity can also be written in terms of the particle mobility,  $B$ , as

$$V_{\text{elec}} = neEB \quad (3-44)$$

or, including the electric charge, in terms of the particle electrical mobility,  $Z = neB$ , as

$$V_{\text{elec}} = ZE \quad (3-45)$$

where the electrical mobility,  $Z$ , is in cm/s per statvolt/cm (or  $\text{cm}^2/\text{statVs}$ ), i.e., unit electrical mobility is a drift velocity of 1 cm/s in a 1 statV/cm field. One statV is equal to 300 volts (V).

### Example 3-6

Foundry fumes are sampled into an electrostatic precipitator for collection onto an electron microscope grid. A power supply is used to apply a potential of 5000 V across the condenser with a plate spacing,  $H$ , of 1 cm. The aerosol flows through the condenser at a uniform velocity of 1 cm/s. The particles of concern have an electrical mobility of  $0.01 \text{ cm}^2/\text{statVs}$ . What is the minimum plate length,  $L$ , that will precipitate all of these particles?

*Answer.* The potential is  $(5000 \text{ V})/(300 \text{ V}/\text{statV}) = 16.7 \text{ statV}$ . The precipitation time,  $t_e$ , in the electric field is

$$\begin{aligned} t_e &= \frac{H}{V_{\text{elec}}} = \frac{H}{ZE} \\ &= \frac{1 \text{ cm}}{\left( 0.01 \frac{\text{cm}^2}{\text{statVs}} \right) \left( \frac{16.7 \text{ statV}}{1 \text{ cm}} \right)} = 6 \text{ s} \end{aligned}$$

The transit time,  $t_t$ , for the air flow at velocity  $U$  must equal or exceed this time:

$$\begin{aligned} t_t &= \frac{L}{U} \geq t_e \\ L &\geq (6 \text{ s})(1 \text{ cm/s}) = 6 \text{ cm} \end{aligned}$$

In SI units, the mobility is converted to  $3.33 \times 10^{-9} \text{ m}^2/\text{V s}$  and the spacing is 0.01 m:

$$t_e = \frac{0.01 \text{ m}}{\left(3.33 \times 10^{-9} \frac{\text{m}^2}{\text{V s}}\right) \left(\frac{5000 \text{ V}}{0.01 \text{ m}}\right)} = 6 \text{ s}$$

The simplest electric field is uniform, e.g., between two large parallel plates

$$E = \frac{\Delta V}{x} \quad (3-46)$$

where  $x$  (cm) is the distance between the plates and  $\Delta V$  is the difference in potential (statV or V). The field between two concentric tubes or between a tube and a concentric wire is also used for electrostatic precipitation. In this case the field is dependent on the distance,  $r$ , from the axis:

$$E = \frac{\Delta V}{r \ln(r_o/r_i)} \quad (3-47)$$

where  $\Delta V$  is the difference in potential between the outer and the inner tube (or wire) of radius  $r_o$  and  $r_i$ , respectively.

The force on each of two particles with  $n_1$  and  $n_2$  unit charges on them is described by Coulomb's law. In cgs units this is

$$F_{\text{elec}} = \frac{n_1 n_2 e^2}{r^2} \quad (3-48)$$

where  $r$  (in cm) is the distance between the particles. This equation applies strictly only to point charges. However, it is a good approximation for the force between two particles or a particle at some distance from a charged object, such as a sampler, and indicates that the force drops off rapidly with distance. Aerosol particles, which typically carry a limited amount of charge because of their small surface area, are, in general, affected electrically only when they are quite close to another charged particle or close to a charged object.

In SI units, Eq. 3-48 is converted to give the force in newtons (N) as

$$F_{\text{elec}} = \frac{n_1 n_2 e^2}{4\pi\epsilon_0 r^2} \quad (3-49)$$

where  $r$  is in meters (m), the electronic charge is  $1.602 \times 10^{-19}$  coulomb (C), and  $\epsilon_0$  is the permittivity constant ( $8.854 \times 10^{-12} \text{ C}^2/\text{N m}^2$  for air or vacuum).

## PARTICLE MOTION IN OTHER FORCE FIELDS

Particle motion is governed by a variety of other forces. Very small particles approach the behavior of the molecules of the surrounding gas, i.e., they diffuse readily and have little inertia and they can be affected by light pressure, acoustic pressure, and thermal pressure. In a fashion similar to gravitational and electrical forces, other forces can be used to cause particle motion and, thus, size-selective measurement. These same forces can also cause particles to be lost rapidly in the sampling inlet or on measurement instrument surfaces. Other forces not mentioned may have some effects but are generally much weaker than the ones mentioned here. For instance, magnetic forces are typically several orders of magnitude smaller than electrostatic forces, but have been used for fiber alignment.

### Thermophoresis

Particles in a thermal gradient are bombarded more strongly by gas molecules on the hotter side and are, therefore, forced away from a heat source. Thus, heated surfaces tend to remain clean, while relatively cool surfaces tend to collect particles. For particles smaller than the mean free path ( $\lambda$ ), the thermophoretic velocity,  $V_{\text{th}}$ , is independent of particle size and is (Waldmann and Schmitt 1966)

$$V_{\text{th}} = \frac{0.55\eta}{\rho_g} \nabla T, \quad d_p < \lambda \quad (3-50)$$

where  $\nabla T$  is the thermal gradient in K/cm. There is a slight increase (of the order of 3%) in the velocity of rough-surfaced particles vs. spherical solids or droplets.

For particles larger than  $\lambda$ , the thermophoretic velocity depends on the ratio of the thermal conductivity of the gas to that of the

particle and also on the particle size. For large conductive aerosol particles, the thermophoretic velocity may be about 5 times lower than for small, nonconductive ones. To calculate the thermophoretic velocity, the molecular accommodation coefficient ( $H$ ) is needed:

$$H \cong \left( \frac{1}{1 + 6\lambda/d_p} \right) \left( \frac{k_g/k_p + 4.4\lambda/d_p}{1 + 2k_g/k_p + 8.8\lambda/d_p} \right) \quad (3-51)$$

where  $k_g$  and  $k_p$  are the thermal conductivities of gas and particle, respectively. The thermal conductivity of air is  $5.6 \times 10^{-5}$  cal/cm s K, while that for particles ranges from 0.16 for a metal (iron) to  $1.9 \times 10^{-5}$  cal/cm s K for an insulator (asbestos) (Mercer 1973, 166). The thermally induced particle velocity is then (Waldmann and Schmitt 1966)

$$V_{th} = \frac{-3\eta H}{2\rho_g T} \nabla T, \quad d_p > \lambda \quad (3-52)$$

Thermophoresis is relatively independent of particle size over a wide range and has been used for collecting small samples, such as for electron microscope measurements, in thermal precipitators. The sampling rate of these instruments is low because of the difficulty of maintaining a thermal gradient and, thus, thermal precipitators have not been scaled up for large volume use.

### Photophoresis

Photophoresis is similar to thermophoresis in that particle motion is caused by thermal gradients at the particle surface except that in this case the heating is caused by light absorption by the particle rather than by an external source. Light shining on a particle may be preferentially absorbed by the side nearer to the light source or, under certain circumstances of weak absorption and focusing, by the far side of the particle. Thus, in the former case the particle will be repelled from the light source while in the latter, called reverse photophoresis, it will be attracted.

### Electromagnetic Radiation Pressure

Electromagnetic radiation can have a direct effect on particle motion by transferring momentum to the particle. Light impinging on a particle can be reflected, refracted or absorbed. The fraction of momentum transfer from the light beam to the particle depends on the geometric cross section of the particle as well as on the average direction of the scattered light. If a significant fraction of the light is absorbed by the particle, photophoresis, as described above, will be more important in deciding particle motion. Radiation pressure has been used to trap particles in focused laser beams and manipulate them for further study.

### Acoustic Pressure

Acoustic waves, either stationary, as in a resonant box, or traveling in open space can be reflected, diffused, or absorbed by particles. Particle motion in an acoustic field includes oscillation in response to the gas motion, circulation in the acoustic field, or net drift in some direction. Such waves have been used to increase particle coagulation or agglomeration or, in other cases, to enhance droplet evaporation or condensation (Hesketh 1977, 97). A resonant acoustic system has also been used to measure particle aerodynamic diameter by measuring a particle's ability to oscillate in response to the air motion (Mazumder et al. 1979).

### Diffusiophoresis and Stephan Flow

When the suspending gas differs in composition from one location to another, diffusion of the gas takes place. This gas diffusion results in suspended particles acquiring a net velocity as a function of the gas diffusion, i.e., diffusiophoresis. The particles are pushed in the direction of the larger molecule flow. The force is a function of the molecular weight and diffusion coefficients of the diffusing gases and is largely independent of particle size.

A special case of diffusiophoresis occurs near evaporating or condensing surfaces. A

net flow of the gas-vapor mixture away from an evaporating surface is set up that creates a drag on particles. The converse situation holds for a condensing surface, i.e., gas and particles will flow towards the surface. This net motion of the gas-vapor mixture is called the Stephan (also spelled Stefan) flow and can cause the motion of particles near these surfaces (Fuchs 1964, 67). The Stephan flow can affect particle collection in industrial scrubbers and scavenging of the environment by growing cloud droplets. In order to increase particle collection by the Stephan flow, the vapor must be supersaturated. Diffusiophoretic velocities are generally only significant for very small particles. For instance, diffusiophoresis of 0.005–0.05  $\mu\text{m}$  diameter particles was found to have the following net deposition velocity,  $V_{\text{diff}}$ , towards surfaces condensing water vapor (Goldsmith and May 1966):

$$V_{\text{diff}} = 1.9 \times 10^{-3} \frac{dP}{dx} \quad (3-53)$$

where the deposition velocity is in cm/s and  $dP/dx$  is the pressure gradient of the diffusing vapor in kPa/cm. Note that in condensing and evaporating droplets, thermophoretic effects can also be important.

## References

- Allen, M. D. and O. G. Raabe. 1985. Slip correction measurements of spherical solid aerosol particles in an improved Millikan apparatus. *Aerosol Sci. Technol.* 4:269–86.
- Barbe-le Borgne, M., D. Boulaud, G. Madelaine, and A. Renoux. 1986. Experimental determination of the dynamic shape factor of the primary sodium peroxide aerosol. *J. Aerosol Sci.* 17:79–86.
- Brockmann, J. E. and D. J. Rader. 1990. APS response to nonspherical particles and experimental determination of dynamic shape factor. *Aerosol Sci. Technol.* 13:162–72.
- Clift, R., J. R. Grace, and M. E. Weber. 1978. *Bubbles Drops and Particles*. New York: Academic Press.
- Davies, C. N. 1945. Definitive equations for the fluid resistance of spheres. *Proc. Phys. Soc.* 57:259.
- Friedlander, S. K. 1977. *Smoke, Dust and Haze*. New York: Wiley.
- Fuchs, N. 1964. *The Mechanics of Aerosols*. Oxford: Pergamon. (Reprinted in 1989, Mineola, NY: Dover.)
- Goldsmith, P. and F. G. May. 1966. In *Aerosol Science*, ed. C. N. Davies. London: Academic Press.
- Hesketh, H. E. 1977. *Fine Particles in Viscous Media*. Ann Arbor: Ann Arbor Science Publishers.
- Hinds, W. C. 1982. *Aerosol Technology*. New York: Wiley.
- Johnson, D. L., D. Leith, and P. C. Reist. 1987. Drag on non-spherical, orthotropic aerosol particles. *J. Aerosol Sci.* 18:87–97.
- Kasper, G., T. Niida, and M. Yang. 1985. Measurements of viscous drag on cylinders and chains of spheres with aspect ratios between 2 and 50. *J. Aerosol Sci.* 16:535–56.
- Licht, W. 1988. *Air Pollution Control Engineering: Basic Calculations for Particulate Collection*. New York: Marcel Dekker.
- Mazumder, M. K., R. E. Ware, J. D. Wilson, R. G. Renninger, F. C. Hiller, P. C. McLeod, R. W. Raible, and M. K. Testerman. 1979. SPART analyzer: Its application to aerodynamic size measurement. *J. Aerosol Sci.* 10:561–69.
- Mercer, T. T. 1973. *Aerosol Technology in Hazard Evaluation*. New York: Academic Press.
- Rader, D. J. 1990. Momentum slip correction factor for small particles in nine common gases. *J. Aerosol Sci.* 21:161–68.
- Sartor, J. D. and C. E. Abbott. 1975. Prediction and measurement of the accelerated motion of water drops in air. *J. Appl. Meteorol.* 14(2):232–39.
- Schlichting, H. 1979. *Boundary-Layer Theory*. New York: McGraw Hill.
- Sheaffer, A. W. 1987. Drag on modified rectangular prisms. *J. Aerosol Sci.* 18:11–16.
- Tsai, C. J. and D. Y. H. Pui. 1990. Numerical study of particle deposition in bends of a circular cross-section—laminar flow regime. *Aerosol Sci. Technol.* 12:813–31.
- Waldmann, L. and K. H. Schmitt. 1966. Thermophoresis and diffusiophoresis of aerosols. In *Aerosol Science*, ed. C. N. Davies. London: Academic Press.
- White, F. M. 1986. *Fluid Mechanics*. New York: McGraw-Hill.
- Willeke, K. 1976. Temperature dependence of particle slip in a gaseous medium. *J. Aerosol Sci.* 7:381–87.

---

# AEROSOL MEASUREMENT

Principles, Techniques, and Applications

Edited by  
Klaus Willeke  
Paul A. Baron



VAN NOSTRAND REINHOLD  
New York